Thicker lubricant layer enhances the droplet mobility on lubricant-infused smooth surfaces.

Ryo Sakai (酒井 遼)[1,2], Takashi Hiroi (廣井 卓思)[3#], Ryota Tamate (玉手　亮多)[4], Timothée Mouterde*[5], and Mizuki Tenjimbayashi (天神林 瑞樹)*[1,2,6]

[1]*Research Center for Materials Nanoarchitectonics (MANA), National Institute for Materials Science (NIMS), 1-1 Namiki, Tsukuba, Ibaraki, 305-0044 Japan*
[2]*Department of Applied Chemistry, Chuo University, Tokyo 112-8551, Japan*
[3]*International Center for Young Scientists (ICYS), NIMS, 1-2-1 Sengen, Tsukuba, 305-0047, Japan*
[4]*Research Center for Macromolecules & Biomaterials, NIMS, 1-2-1 Sengen, Tsukuba, 305-0047, Japan*
[5]*Department of Mechanical Engineering, The University of Tokyo, 7-3-1 Hongo, Bunkyo-ku, Tokyo 113-8656, Japan*
[6]*FOREST, Japan Science and Technology Agency, Saitama 332-0012, Japan*
**Correspondance to T.M. <mouterde@g.ecc.u-tokyo.ac.jp> and M.T. < TENJIMBAYASHI.Mizuki@nims.go.jp>*
[#]*Present address: School of Advanced Science and Engineering, Waseda University, 3-4-1 Okubo, Shinjuku-ku, Tokyo 169-8555, Japan*

Abstract

Droplets are highly mobile on lubricant-infused surfaces when droplet−lubricant phases are immiscible and lubricant layer is stable. Recent studies have shown that the high droplet mobility is due to absence of three-phase contact line friction by oleoplaning of the droplets on the lubricant layer. In this state, dynamic friction arises primarily from viscous dissipation in the lubricant around the droplet. Classical Landau–Levich–Derjaguin (LLD) law suggests that the friction force is proportional to the two-thirds power of the capillary number, and the lubricant thickness effect is not included. Here, we discovered that increased lubricant thickness enhances the droplet's mobility on lubricant-infused surfaces. This finding is unexpected, as a thicker lubricant layer would typically increase the potential volume for viscous dissipation. We formed stable lubricant layers of varying thicknesses ranging from tens to hundreds of micrometers on a "nanometrically smooth" base layer to remove the influence of surface texture. The droplet friction force on the different lubricant thickness surfaces is measured using the cantilever method. While all surfaces follow LLD law, the friction force significantly decreases with increasing the lubricant thicknesses. The possible reason is the decrement of the energy dissipation at the lubricant ridge with the thickness. We propose a modified friction model incorporating the thickness dependence with the classical law, offering deeper insight into droplet friction dynamics on the lubricant-infused surfaces. In practical terms, reducing droplet friction enhances transport efficiency, contributing to advancements in fluidic systems and liquid-repellent applications.

Minimizing energy dissipation during droplet motion on engineered surfaces is essential for effective small liquid volumes manipulation.[1,2] Various liquid-repellent surfaces have been reported, including superhydrophobic,[3] superoleophobic,[4] liquid-like,[5,6] and lubricant-infused surfaces.[7,8] Lubricant-infused surfaces have been widely studied due to their high droplet mobility, pressure stability, and self-repairing omniphobicity. Lubricant-infused surfaces comprise the top lubricant layer and textured base solid layer for immobilizing the lubricant onto the substrate. When the droplet is immiscible with the lubricant and does not preferentially wet the substrate, the droplet becomes highly mobile, and exhibiting slippery behavior . Various works studied the effect of the droplet mobility on the lubricant-infused surfaces.[9,10] Smith *et al.* studied the general condition for interfacial stability of droplets on the lubricant-infused surfaces.[11] The interfacial states are directly observed by Schellenberger *et al*.[12] Their dynamics have been studied by Daniel *et al.,* who found that moving droplets are oleoplaning on the lubricant films, which prevents the formation of the contact line between the droplet, textured base solid, and the lubricant.[13,14] In this case, the droplet friction force originates from the viscous dissipation of the lubricant around the droplet. They proposed general friction laws depending on whether the lubricant thickness beneath the droplet is greater than or less than the texture height. Keiser *et al.* further examined the sources of viscous dissipation around the droplet.[15] They demonstrated that the main dissipation source is in the droplet front and rear wetting ridges, specifically at the air−lubricant and lubricant−water interfaces. Additionally, they confirmed the effect of the texture height on the droplet friction. Moreover, several efforts to control the lubricant shape and thickness distribution by patterning,[16,17] substrate shape,[18] or external stimuli[19] to enhance the mobility of droplets have been reported. Here, we questioned the impact of the lubricant thickness on the droplet friction. While the lubricant amount around the droplet increases with its thickness, the wetting ridge should gradually disappear.[20,21] According to the numerical study by Naga *et al.*,[22] the energy dissipation at the wetting ridge is not small. Thus, we expect the thicker lubricant layer can decrease the droplet friction. Actually, Guo *et al*. predict the lubricant thickness may increase a droplet mobility on the lubricant-infused surface in their numerical study.[23]

However, the direct impact of the lubricant thickness on droplet mobility remains unclear. The requirement of the textured solid base layer makes studying the effect of the lubricant thickness challenging. Recent studies have reported the design of lubricant-infused surfaces on smooth base layers.[24–27] In these works, the different non-covalent interactions between the lubricant and base layers are applied to form stable lubricant-infused surfaces. We also We also reported the stabilization of silicone oil film on phenylsilane-modified glass substrates with a surface roughness below 1 nm by tuning

the molecular interactions between the lubricant and the base layer.[25] Thus, our surface would be a tool to study the droplet friction without lubricant thickness limit due to the structure. The resulting surface exhibits high droplet mobility, with droplets advancing and receding without pining (**Fig 1(a)**), similar to typical slippery surfaces. This lubricant-infused smooth surface provides a powerful tool for studying how the lubricant thickness affects droplet mobility, which is the focus of this work.

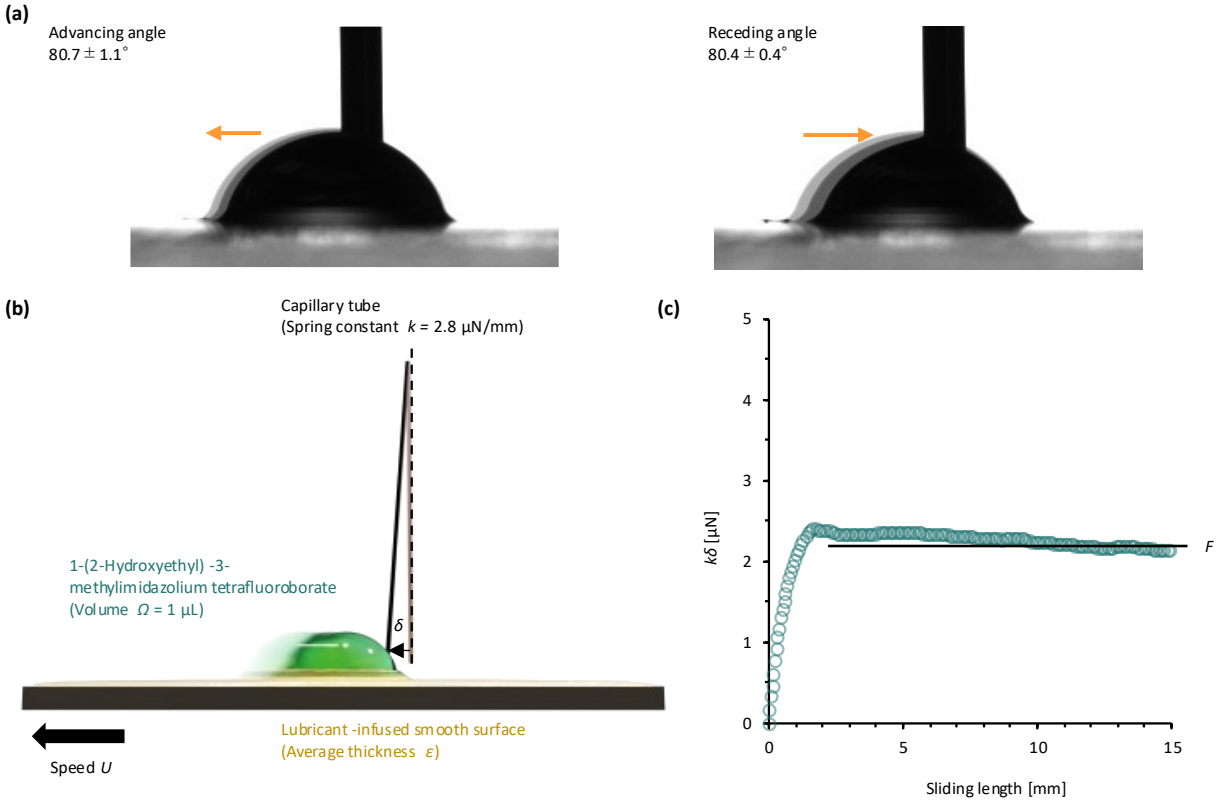

FIG. 1. (a) Droplet advancing/receding behavior on the lubricant-infused smooth surface. The negligibly small dynamic contact angle values make droplet friction force measurement difficult.[27] **(b)** Experimental setup for droplet friction force measurement. A 1 μL ionic liquid droplet is placed on the lubricated surface, which is translated horizontally with a velocity U. A cantilever with spring constant $k = 2.8 \pm 0.1$ μN/mm is inserted inside the droplet, and its deflection allows to measure the friction force F experienced by the droplet on the surface. **(c)** Typical dissipation force curve F plotted as a function of the sliding length for a lubricant layer $\varepsilon = 105$ μm and sliding velocity $U = 0.5$ mm/s.

However, small contact angle hysteresis on the lubricated surface (**Fig 1(a)**) makes droplet friction force measurement difficult. Thus, the experimental setup was carefully designed (**Fig. 1(b)**) to enable accurate measurement of droplet friction. Following the protocol developed in our previous study,[25] we coat a phenylsilane-modified nanometrically smooth glass substrate with silicone oil (Surface tension: γ_l = 20 mN/m and viscosity: η = 46.5 mPa·s). Here, we confirmed that the lubricant is a Newtonian fluid, as its viscosity does not depend on the shear rate (**Fig. S1**). The lubricant thickness ε, estimated by direct mass measurement using the relation $\varepsilon = \rho\Delta m/S$ (ρ: lubricant density, Δm: mass increase after coating, S: coated area), is controlled by the shearing force through spin coating. The resolution of Δm is ± 0.01 mg using a microbalance (BA-225DTE, A&D Company, Limited, Japan). We used the substrate size of 6.7 ± 0.1 cm^2, and the theoretical thickness error by this measurement is *c.a.* ρ(error of Δm)/S ~ 0.01 μm. However, the lubricant thickness is not plateau near the edge. Thus, we conducted the force measurement on the plateau region. In this work, we investigate the effect of the lubricant thickness on the friction of droplets on the liquid-infused smooth surface for thicknesses ranging from tens to hundreds of micrometers. When the lubricant thickness is decreased to ε = 2.1 μm, lubricant is too thin to remain stable and uniform (**Fig. S2**). A 1 μL ionic liquid droplet 1-(2-Hydroxyethyl)-3-methylimidazolium tetrafluoroborate ([C_2mimOH][BF4]) with surface tension γ_d = 58 mN/m and density of 1.34 g/cm³ is used as a probe droplet. Owing to the non-volatility of the ionic liquid, we can neglect the droplet evaporation effects during the experiments. Here, bond number considering lubricant and ionic liquid densities is Bo = $\Delta\rho g L^2/\gamma_{dl}$ is 1.8×10^{-4}, and the droplet shape is not distorted by the gravity ($\Delta\rho$ is density difference between droplet and lubricant, g is gravitational acceleration constant, L is characteristic length estimated by the droplet diameter ~1 mm, and γ_{dl} = 19 mN/m the droplet−lubricant interfacial tension). The droplet is deposited on the lubricated surface and attached to a glass capillary cantilever with spring constant k = 2.8 ± 0.1 μN/mm measured by Daniel's method (**Fig. S3**).[13] Then, the lubricated substrate is translated horizontally by a motorized stage with the velocity U (ranging from 2 μm/s to 1 mm/s). In this velocity, Reynolds number Re = $\rho UL/\eta$ ranges from 10^{-4} to 10^{-2} and the inertia effect is negligibly small compared with viscous effect. Using a camera, we record the deflection δ of the cantilever from its initial position, which allows us to measure the friction force $F = k\delta$ for different velocities. **Figure 1(c)** shows a typical force curve plotted as a function of the substrate displacement (here ε = 105 μm and U = 0.5 mm/s). We observe that the droplet experiences a static friction-like dissipation, which then transitions to a plateau, the average value of which corresponds to the dynamic friction force F that we are now studying.

We first investigate whether a droplet on liquid-infused smooth surfaces obeys the classical LLD law observed for lubricant-infused textured surfaces to test if a textured base is essential for the observed scaling; that is, $F \sim \mathrm{Ca}^{2/3}$ when the lubricant layer beneath the droplet is thicker than the texture height ($\mathrm{Ca} = \eta U/\gamma_{\mathrm{dl}}$ is the capillary number).[13,15,28] We plot in **Figure 2** the evolution of F as a function of Ca on double logarithmic coordinates, for lubricant layers with thicknesses ranging from 18 to 400 µm. We find that the friction follows a power law: $F \sim \mathrm{Ca}^{2/3}$ for all plots, indicating that friction on liquid-infused smooth surfaces obeys the same LLD law as observed on liquid-infused textured surfaces.

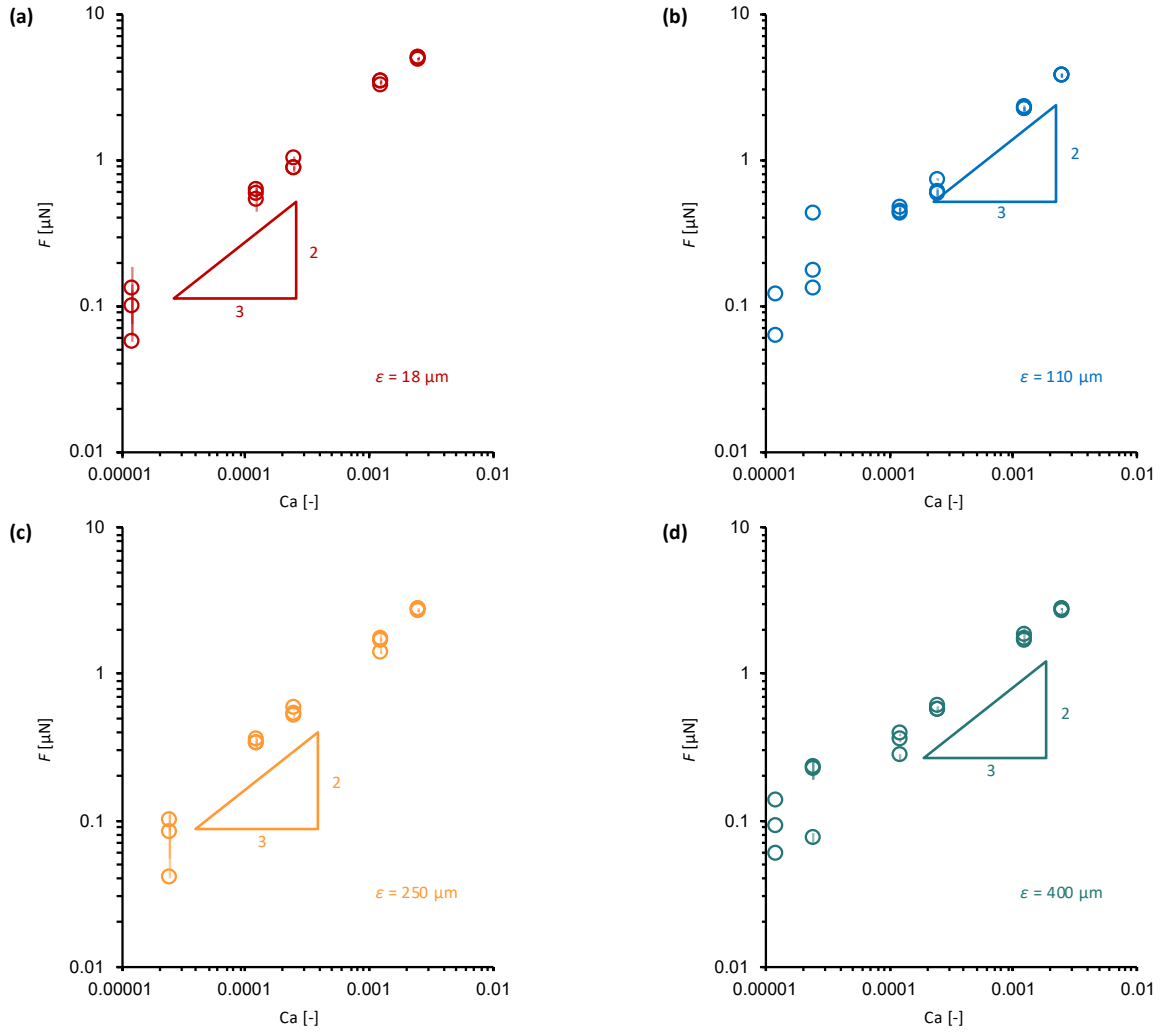

FIG. 2. Dynamic friction force of 1 µL ionic liquid droplets on liquid-infused smooth surfaces plotted as a function of the Capillary number in log-log coordinates. A slope of 2/3, characteristic of the LLD friction law, is shown on each plot. **(a)** ε = 18 µm, **(b)** ε = 110 µm, **(c)** ε = 250 µm, and **(d)** ε = 400 µm.

The amount of lubricant surrounding the droplet visibly increases with ε (**Figure 3**). The shape difference of the lubricant ridge around the droplet corresponds to the lubricant pressure.[20] However, as shown in **Figures 4(a)** and **4(b)**, in which we plot the dissipation force as a function of the lubricant layer thickness at fixed capillary numbers, the friction force decreases as the lubricant thickness increases, eventually reaching a plateau for thicknesses greater than ~100 μm. Notably, the thickness dependence of the dissipation force is not captured by current friction models,[13,15,28] although the observed lubricant shape around the droplet is apparently different (**Figure 3**). We now propose a modified friction law that incorporates lubricant thickness; because existing models do not account for the frictional behavior when lubricant thickness is decoupled from substrate texture, as in our liquid infused smooth surface. Contrary to previous works,[13,15,28] the lubricant thickness is not maintained by surface textures, which modifies the droplet's friction. In our case, the droplet motion is no longer constrained by the underlying surface due to the absence of the base layer texture. We consider the six possible regions for friction by viscous dissipation as proposed by Keiser *et al*. (**Fig. 4(c)**). We evaluate how the texture's absence and the lubricant layer thickness affect the drop dissipation force. The dissipation can originate from the lubricant foot, with advancing (regions 1 and 3) and receding (regions 2 and 4) sides, from viscous dissipation inside the droplet (region 6) or in the lubricant film below the drop (region 5). As shown in previous studies,[13–15,22] the dissipation in regions 5 and 6 is negligible for droplets with viscosity much lower than that of the lubricant. Indeed, the rotation of the liquid inside the droplet minimizes the velocity at the lubricant/droplet interface, which reduces the velocity gradients within the lubricant layer (region 5). The dissipation inside the droplet (region 6) scales as Ca, which in the small capillary number regime is always negligible when compared to other dissipations scaling as $Ca^{2/3}$. Without the surface texture, the dissipations in the menisci of regions 2 and 3 are the same.[15,22] Assuming a LLD model and denoting $R \approx 0.78$ mm as the droplet contact radius, the film thickness is estimated as $e \sim R\mathrm{Ca}^{2/3}$, and the dynamic meniscus length writes $l \sim R\mathrm{Ca}^{1/3}$. The viscous stress $\eta U/e$, integrated over the meniscus surface, gives the dissipation: $F_{2/3} \sim (\eta U/e)lR \sim \gamma_{dl} R\mathrm{Ca}^{2/3}$, which indicates that this component of the dissipation is independent of the initial lubricant thickness ε. We will now focus the dissipations in the regions 1 and 4.

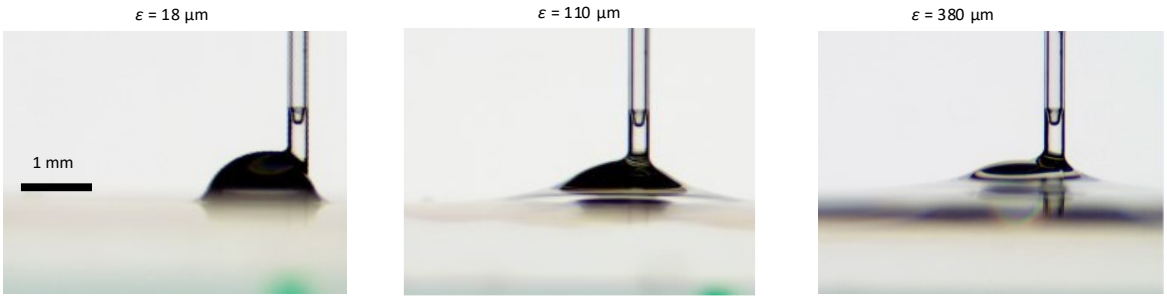

FIG. 3. Side view photos of the droplet on the lubricated surfaces with different lubricant thicknesses.

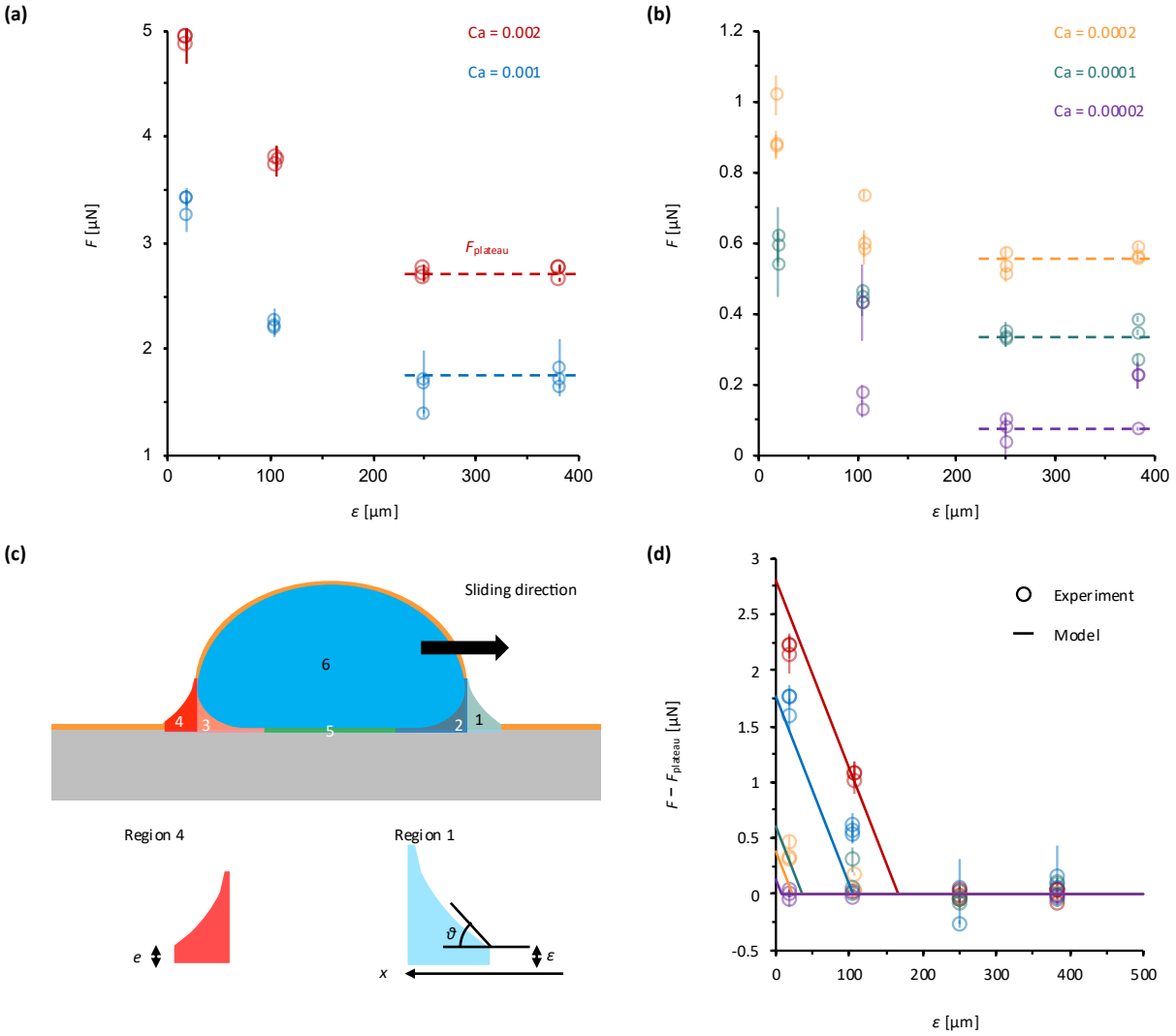

FIG. 4. (a, b) Dissipation force F plotted as a function of the lubricant thickness ε at different capillary numbers. **(c)** Sketch of the droplet sliding on the lubricant layer with the six possible dissipation regions. The regions 1 and 4, relevant to this case, are highlighted below. **(d)** Friction force F, to which the force plateau value is subtracted and plotted as a function of the lubricant thickness ε. The model for F_4 is plotted for each capillary number with a plain line.

In region 1, we denote x the distance from the meniscus tip where the thickness is minimal given by ε **(Fig. 4(c))**. When the foot advances, it forms a dynamic contact angle θ, which controls the slope of thickness variations so that the meniscus thickness for small θ writes $h = \varepsilon + \theta x$. The total viscous friction in region 1 then writes: $F_1 \sim \int(\eta U/(\varepsilon + \theta x)R\mathrm{d}x$, which we integrate for x varying from a molecular cut-off scale b (to account for the limit case $\varepsilon = 0$), to a, the meniscus length ~ 100 µm. The friction force then writes: $F_1 \sim \eta UR/\theta \ \mathrm{In}[(\varepsilon + \theta a)/(\ \varepsilon + \theta b)]$.

We then evaluate two limit cases. In the first case, when $\varepsilon << \theta a$, θb, the logarithm becomes independent of θ. Balancing F_1 with the capillary force $\mathrm{g}R(1 - \cos\theta) \sim \mathrm{g}R\theta^2/2$ gives Tanner's law $\theta \sim \mathrm{Ca}^{1/3}$ and, finally, the expression of the force:[15,29] $F_1 \sim \gamma_\mathrm{d} R\mathrm{Ca}^{2/3}\ \ln^{2/3}(b/a)$. This case should hold for very thin lubricant thickness or large capillary number to satisfy $\mathrm{Ca} > (\varepsilon/a)^3$. The opposite case $\varepsilon >> \theta a$, θb, is relevant to the range of thicknesses explored in our study. We simplify the equation for F_1 by neglecting θb over ε and taking a first-order Taylor expansion of the logarithm: $\ln(1+ \theta a/\varepsilon) \sim \theta a/\varepsilon$, we obtain $F_1 \sim \gamma_\mathrm{d} R\mathrm{Ca}\ (a/\varepsilon)$. While this dissipation decreases with increasing thickness, its linear dependency on Ca is always negligible compared to the other dissipation sources scaling with $\mathrm{Ca}^{2/3}$. Hence, this cannot explain the decrease of friction observed experimentally.

In region 4, a LLD film may be formed, resulting in a film thickness e. Depending on this thickness, we distinguish two cases. When the drop moves sufficiently slowly to avoid forming a LLD film thicker than ε, the viscous dissipation is similar to that of the front region 1 for thick layers, and we have $F_4 \sim \gamma_\mathrm{d} R\mathrm{Ca}\ (a/\varepsilon)$. As discussed for region 1, the linear dependency on capillary numbers makes this contribution negligible compared to other frictions for the capillary numbers explored. Next, we evaluate the case of the droplet being fast enough to form a LLD film thicker than ε ($e > \varepsilon$). The presence of an existing lubricant layer modifies the LLD film. We propose a modified scaling law for the LLD film in the presence of an existing lubricant layer with thickness ε. The change of thickness $(e - \varepsilon)$, over a distance l —the dynamic meniscus extension—creates a capillary pressure gradient $\gamma_\mathrm{l}(e - \varepsilon)/l^3$. By balancing it with the viscous volume force $\eta U/e^2$, we obtain $l/e \sim \mathrm{Ca}_\mathrm{l}^{-1/3}(1 - \varepsilon/e)^{1/3}$, where $\mathrm{Ca}_\mathrm{l} = \eta U/\gamma_\mathrm{l}$ is the lubricant capillary number. Matching the static

meniscus curvature κ with the dynamic one $(e - \varepsilon)/l^2$ gives a relation for the thickness $e \sim \kappa^{-1}\mathrm{Ca}_l^{2/3}\ (1 - \varepsilon/e)^{1/3}$. This equation shows that the total thickness is reduced compared with the case without a pre-existing lubricant layer. To solve this 4th-order equation in e, we assume $\varepsilon/e << 1$ and take the first-order Taylor expansion of the right-hand side; this reduces the problem to a second-order equation in which the largest root is given by $e = \kappa^{-1}\mathrm{Ca}_l^{2/3} - \varepsilon/3$. For thin lubricant layers (ε approaching 0), we obtain the standard LLD scaling. Interestingly, this model predicts a reduction of the deposited thickness, as the dynamic meniscus curvature, which limits the film deposition, is reduced by the smaller thickness variation. From this simple model, we derive the viscous friction. As previously described for regions 2 and 3, we integrate the viscous stress ($\eta U/e$) over the meniscus surface lR and we obtain: $F_4 \sim \eta UR(l/e) \sim \pi\gamma_d R(\mathrm{Ca}_l^{2/3} - \varepsilon/3\kappa^{-1})$. This equation first predicts that the friction should decrease linearly with the lubricant thickness and, for a given capillary number, it should become zero for a lubricant thickness $\varepsilon \approx 3\kappa^{-1}\mathrm{Ca}_l^{2/3}$. To test our prediction, we plot in **Fig. 4(d)** the dissipation $F - F_{\mathrm{plateau}}$, where F_{plateau} is the plateau value of the friction force obtained in the regime independent of the lubricant thickness, $\varepsilon > 200$ μm (**Fig. 4(a)** and **4(b)**). We adjust the amplitude of our model with a coefficient of 3.6 (of order 1), and the model is well adjusted with a static film radius of curvature $\kappa^{-1} \approx 3.5$ mm for all capillary numbers, a value in reasonable agreement with experiments. The model is plotted for each capillary number with a plain line in **Fig. 4(d)** and show a qualitative agreement with the experimental data. Our prediction captures the decrease of the friction with increasing lubricant layer thickness, the existence of a critical thickness at which this dissipation vanishes. This prediction identifies a critical design parameter for maximizing droplet mobility in lubrication-based systems. Also, the correction term $\varepsilon/3\kappa^{-1}$ is negligible for small thicknesses, which explains why it was not observed in previous studies.[13]

In summary, we showed that droplets on liquid-infused smooth surfaces follow the same friction law as on liquid-infused textured surfaces $\sim \mathrm{Ca}^{2/3}$, despite the absence of texture. We then discovered that the friction decreases with increasing lubricant thickness. We proposed a model based on a modified LLD law, which captures the effect of the lubricant thickness. This study not only confirms that droplet friction on lubricant-infused smooth surface follows the classical LLD law, but also introduces a revised model that captures friction reduction with increasing lubricant thickness, an effect absent in previous models relying on textured substrates. Moreover, our findings also offer a better understanding of general friction dynamics, as the interfacial shape evolution is a ubiquitous feature in various friction processes.[30] Increasing the lubricant thickness is a simple but versatile strategy to enhance the droplet mobility on the lubricated surface. However, the strategy cannot be applied to solid liquid-repellent surfaces.[31] A highly mobile droplet on a surface can lead to various potential applications relating to droplet transportation.

SUPPLEMENTARY MATERIAL

See the supplementary material for the lubricant rheology, lubricant layer images, and measurement of the spring constant of the cantilever.

This work was supported by World Premier International Research Center Initiative (WPI), MEXT, Japan. This work was partially supported by JSPS KAKENHI (21H01643, 23K18567, 24K01341), JSPS LEADER, JST FOREST (JPMJFR223V), and TIA KAKEHASHI.

AUTHOR DECLARATIONS

Conflict of Interest

The authors have no conflicts to disclose.

Author Contributions

M.T. and T.M. supervised the project, acquired the funding, and designed the experiment. T.M. built the model. R.S. conducted the experiment. M.T., T.M., and R.S. analyzed the data. T.H. and R.S. designed the force measurement setup. R.T. conducted rheology measurement. M.T. and T.M. wrote the paper.

DATA AVAILABILITY

The data that support the findings of this study are available within the article.

REFERENCES

[1] J. Xu, S. Xiu, Z. Lian, H. Yu, and J. Cao, "Bioinspired materials for droplet manipulation: Principles, methods and applications," Droplet **1**(1), 11–37 (2022).
[2] M. Tenjimbayashi, and K. Manabe, "A review on control of droplet motion based on wettability modulation: principles, design strategies, recent progress, and applications," Sci Technol Adv Mater **23**(1), 473–497 (2022).
[3] S. Shibuichi, T. Onda, N. Satoh, and K. Tsujii, "Super Water-Repellent Surfaces Resulting from Fractal Structure," J Phys Chem **100**(50), 19512–19517 (1996).
[4] A. Tuteja, W. Choi, J.M. Mabry, G.H. McKinley, and R.E. Cohen, "Robust omniphobic surfaces," Proceedings of the National Academy of Sciences **105**(47), 18200–18205 (2008).

[5] D.F. Cheng, C. Urata, M. Yagihashi, and A. Hozumi, "A Statically Oleophilic but Dynamically Oleophobic Smooth Nonperfluorinated Surface," Angewandte Chemie International Edition **51**(12), 2956–2959 (2012).
[6] L. Wang, and T.J. McCarthy, "Covalently Attached Liquids: Instant Omniphobic Surfaces with Unprecedented Repellency," Angewandte Chemie International Edition **55**(1), 244–248 (2016).
[7] A. Lafuma, and D. Quéré, "Slippery pre-suffused surfaces," EPL (Europhysics Letters) **96**(5), 56001 (2011).
[8] T.-S. Wong, S.H. Kang, S.K.Y. Tang, E.J. Smythe, B.D. Hatton, A. Grinthal, and J. Aizenberg, "Bioinspired self-repairing slippery surfaces with pressure-stable omniphobicity," Nature **477**(7365), 443–447 (2011).
[9] S. Hardt, and G. McHale, "Flow and Drop Transport Along Liquid-Infused Surfaces," Annu Rev Fluid Mech **54**(1), 83–104 (2022).
[10] E. Bormashenko, "Physics of pre-wetted, lubricated and impregnated surfaces: a review," Philosophical Transactions of the Royal Society A: Mathematical, Physical and Engineering Sciences **377**(2138), 20180264 (2019).
[11] J.D. Smith, R. Dhiman, S. Anand, E. Reza-Garduno, R.E. Cohen, G.H. McKinley, and K.K. Varanasi, "Droplet mobility on lubricant-impregnated surfaces," Soft Matter **9**(6), 1772–1780 (2013).
[12] F. Schellenberger, J. Xie, N. Encinas, A. Hardy, M. Klapper, P. Papadopoulos, H.-J. Butt, and D. Vollmer, "Direct observation of drops on slippery lubricant-infused surfaces," Soft Matter **11**(38), 7617–7626 (2015).
[13] D. Daniel, J.V.I. Timonen, R. Li, S.J. Velling, and J. Aizenberg, "Oleoplaning droplets on lubricated surfaces," Nat Phys **13**(10), 1020–1025 (2017).
[14] M.J. Kreder, D. Daniel, A. Tetreault, Z. Cao, B. Lemaire, J.V.I. Timonen, and J. Aizenberg, "Film Dynamics and Lubricant Depletion by Droplets Moving on Lubricated Surfaces," Phys Rev X **8**(3), 031053 (2018).
[15] A. Keiser, P. Baumli, D. Vollmer, and D. Quéré, "Universality of friction laws on liquid-infused materials," Phys Rev Fluids **5**(1), 014005 (2020).
[16] M.S. Sadullah, G. Launay, J. Parle, R. Ledesma-Aguilar, Y. Gizaw, G. McHale, G.G. Wells, and H. Kusumaatmaja, "Bidirectional motion of droplets on gradient liquid infused surfaces," Commun Phys **3**(1), 166 (2020).
[17] J. Hui Guan, É. Ruiz-Gutiérrez, B. Bin Xu, D. Wood, G. McHale, R. Ledesma-Aguilar, and G. George Wells, "Drop transport and positioning on lubricant-impregnated surfaces," Soft Matter **13**(18), 3404–3410 (2017).
[18] B. V. Orme, G. McHale, R. Ledesma-Aguilar, and G.G. Wells, "Droplet Retention and Shedding on Slippery Substrates," Langmuir **35**(28), 9146–9151 (2019).
[19] U. Banerjee, M.R. Gunjan, and S.K. Mitra, "Directional Manipulation of Drops and Solids on a Magneto-Responsive Slippery Surface," Langmuir **40**(6), 3105–3116 (2024).
[20] C. Semprebon, G. McHale, and H. Kusumaatmaja, "Apparent contact angle and contact angle hysteresis on liquid infused surfaces," Soft Matter **13**(1), 101–110 (2017).
[21] R. Üçüncüoğlu, and H.Y. Erbil, "Water Drop Evaporation on Slippery Liquid-Infused Porous Surfaces (SLIPS): Effect of Lubricant Thickness, Viscosity, Ridge Height, and Pattern Geometry," Langmuir **39**(18), 6514–6528 (2023).
[22] A. Naga, M. Rennick, L. Hauer, W.S.Y. Wong, A. Sharifi-Aghili, D. Vollmer, and H. Kusumaatmaja, "Direct visualization of viscous dissipation and wetting ridge geometry on lubricant-infused surfaces," Commun Phys **7**(1), 306 (2024).
[23] L. Guo, G.H. Tang, and S. Kumar, "Droplet Morphology and Mobility on Lubricant-Impregnated Surfaces: A Molecular Dynamics Study," Langmuir **35**(49), 16377–16387 (2019).

[24] D.C. Leslie, A. Waterhouse, J.B. Berthet, T.M. Valentin, A.L. Watters, A. Jain, P. Kim, B.D. Hatton, A. Nedder, K. Donovan, E.H. Super, C. Howell, C.P. Johnson, T.L. Vu, D.E. Bolgen, S. Rifai, A.R. Hansen, M. Aizenberg, M. Super, J. Aizenberg, and D.E. Ingber, "A bioinspired omniphobic surface coating on medical devices prevents thrombosis and biofouling," Nat Biotechnol **32**(11), 1134–1140 (2014).
[25] M. Tenjimbayashi, R. Togasawa, K. Manabe, T. Matsubayashi, T. Moriya, M. Komine, and S. Shiratori, "Liquid-Infused Smooth Coating with Transparency, Super-Durability, and Extraordinary Hydrophobicity," Adv Funct Mater **26**(37), 6693–6702 (2016).
[26] J. Wang, L. Wang, N. Sun, R. Tierney, H. Li, M. Corsetti, L. Williams, P.K. Wong, and T.-S. Wong, "Viscoelastic solid-repellent coatings for extreme water saving and global sanitation," Nat Sustain **2**(12), 1097–1105 (2019).
[27] R. Samanta, and S. Rowthu, "Can Microcavitated Slippery Surfaces Outperform Micropillared and Untextured?," Langmuir **40**(42), 22324–22337 (2024).
[28] K. Yamamoto, S. Takagi, Y. Ichikawa, and M. Motosuke, "Lubrication effects on droplet manipulation by electrowetting-on-dielectric (EWOD)," J Appl Phys **132**(20), (2022).
[29] L.H. Tanner, "The spreading of silicone oil drops on horizontal surfaces," J Phys D Appl Phys **12**(9), 1473–1484 (1979).
[30] S. Jin, X. Li, H. Gao, P. Wang, and D. Zhang, "Analysis and Prospects of Lubrication and Friction Characteristics in Cold Strip Rolling: A Review," Steel Res Int **96**(1), 1–19 (2025).
[31] X. Li, F. Bodziony, M. Yin, H. Marschall, R. Berger, and H.-J. Butt, "Kinetic drop friction," Nat Commun **14**(1), 4571 (2023).